Coordinate regulation of neutrophil homeostasis by liver X receptors in mice

Cynthia Hong,[1,2] Yoko Kidani,[1,3] Noelia A-Gonzalez,[4] Tram Phung,[1,3] Ayaka Ito,[1,2] Xin Rong,[1] Katrin Ericson,[5] Hanna Mikkola,[5] Simon W. Beaven,[2] Lloyd S. Miller,[6] Wen-Hai Shao,[7] Philip L. Cohen,[7] Antonio Castrillo,[4,8] Peter Tontonoz,[1,2] and Steven J. Bensinger[1,3]

[1]Department of Pathology and Laboratory Medicine, David Geffen School of Medicine, UCLA, Los Angeles, California, USA. [2]Howard Hughes Medical Institute, UCLA, Los Angeles, California, USA. [3]Institute for Molecular Medicine, David Geffen School of Medicine, UCLA, Los Angeles, California, USA. [4]Immune Signaling Laboratory, Department of Biochemistry and Molecular Biology: School of Medicine, University of Las Palmas, Las Palmas, Spain. [5]Department of Molecular, Cell, and Developmental Biology, UCLA, Los Angeles, California, USA. [6]Department of Medicine, Division of Dermatology, David Geffen School of Medicine, UCLA, Los Angeles, California, USA. [7]Department of Medicine, Section of Rheumatology, Temple University School of Medicine, Philadelphia, Pennsylvania, USA. [8]Instituto de Investigaciones Biomedicas "Alberto Sols," Consejo Superior de Investigaciones Cientificas-Universidad Autonoma de Madrid, Madrid, Spain.

The most abundant immune cell type is the neutrophil, a key first responder after pathogen invasion. Neutrophil numbers in the periphery are tightly regulated to prevent opportunistic infections and aberrant inflammation. In healthy individuals, more than 1×10^9 neutrophils per kilogram body weight are released from the bone marrow every 24 hours. To maintain homeostatic levels, an equivalent number of senescent cells must be cleared from circulation. Recent studies indicate that clearance of senescent neutrophils by resident tissue macrophages and DCs helps to set homeostatic levels of neutrophils via effects on the IL-23/IL-17/G-CSF cytokine axis, which stimulates neutrophil production in the bone marrow. However, the molecular events in phagocytes underlying this feedback loop have remained indeterminate. Liver X receptors (LXRs) are members of the nuclear receptor superfamily that regulate both lipid metabolic and inflammatory gene expression. Here, we demonstrate that LXRs contribute to the control of neutrophil homeostasis. Using gain- and loss-of-function models, we found that LXR signaling regulated the efficient clearance of senescent neutrophils by peripheral tissue APCs in a Mer-dependent manner. Furthermore, activation of LXR by engulfed neutrophils directly repressed the IL-23/IL-17/G-CSF granulopoietic cytokine cascade. These results provide mechanistic insight into the molecular events orchestrating neutrophil homeostasis and advance our understanding of LXRs as integrators of phagocyte function, lipid metabolism, and cytokine gene expression.

Introduction

Neutrophils are the most abundant cell type in the immune system and play critical roles in host defense against pathogens. In healthy individuals, neutrophil half-life is exceedingly short, with estimates ranging from 3–12 h in a variety of animal and human studies (1–5). It has been estimated that 10^9–10^{11} neutrophils are released into the circulation from the bone marrow on a daily basis (6). Accordingly, an equivalent number of senescent neutrophils must be removed from the circulation to maintain homeostasis. Apoptotic or aged neutrophils are cleared primarily by resident tissue macrophages in the liver, spleen, and bone marrow (7–11). Perturbation of peripheral neutrophil homeostasis affects innate and adaptive immunity and may result in life threatening infections or autoinflammatory/autoimmune disease. Thus, understanding the mechanisms that regulate granulopoiesis, release and clearance of neutrophils is of interest to the immunologic, infectious disease, rheumatology and cancer fields.

An important feedback relationship between peripheral clearance of apoptotic neutrophils and bone marrow release has recently been uncovered. Ley and colleagues have shown that extravasation and phagocytosis of apoptotic neutrophils in the spleen and liver regulates granulocyte release from the bone marrow (10, 12). Examination of genetic models deficient in leukocyte extravasation revealed that phagocytosis of apoptotic neutrophils represses expression of IL-23 by resident tissue macrophages and DCs. In the absence of efficient phagocytosis, IL-23 production is elevated, resulting in the secretion of IL-17 from αβ and γδ T cells. In turn, IL-17 induces G-CSF production in the bone marrow that stimulates granulopoiesis and efflux from the bone marrow (10, 12, 13). Although it is clear that phagocytosis of apoptotic neutrophils negatively regulates IL-23 production, the molecular mechanism by which engulfment of senescent neutrophils quells IL-23 production remains largely unknown.

Liver X receptor α (LXRα) and LXRβ (encoded by *Nr1h3* and *Nr1h2*, respectively) are oxysterol-activated nuclear receptors that regulate cholesterol homeostasis (14, 15). Activation of LXRs drives the expression of genes involved in reverse cholesterol transport, biliary excretion and intestinal absorption (16). In addition, LXR signaling negatively regulates inflammation via repression of inflammatory gene expression (17, 18). LXRs have emerged as modulators of inflammation in an array of metabolic, inflammatory, infectious and autoimmune diseases (17, 19–25). Despite advances in understanding the mechanisms of LXR-dependent lipid metabolic and inflammatory gene regulation, it remains unclear why these 2 processes should be tightly linked in innate immune cells. Herein, we report that LXRs play a previously unrecognized role in controlling peripheral neutrophil homeostasis via the coordinate regulation of senescent neutrophil clearance and granulopoietic cytokine expression.

Conflict of interest: The authors have declared that no conflict of interest exists.

Citation for this article: *J Clin Invest.* 2012;122(1):337–347. doi:10.1172/JCI58393.

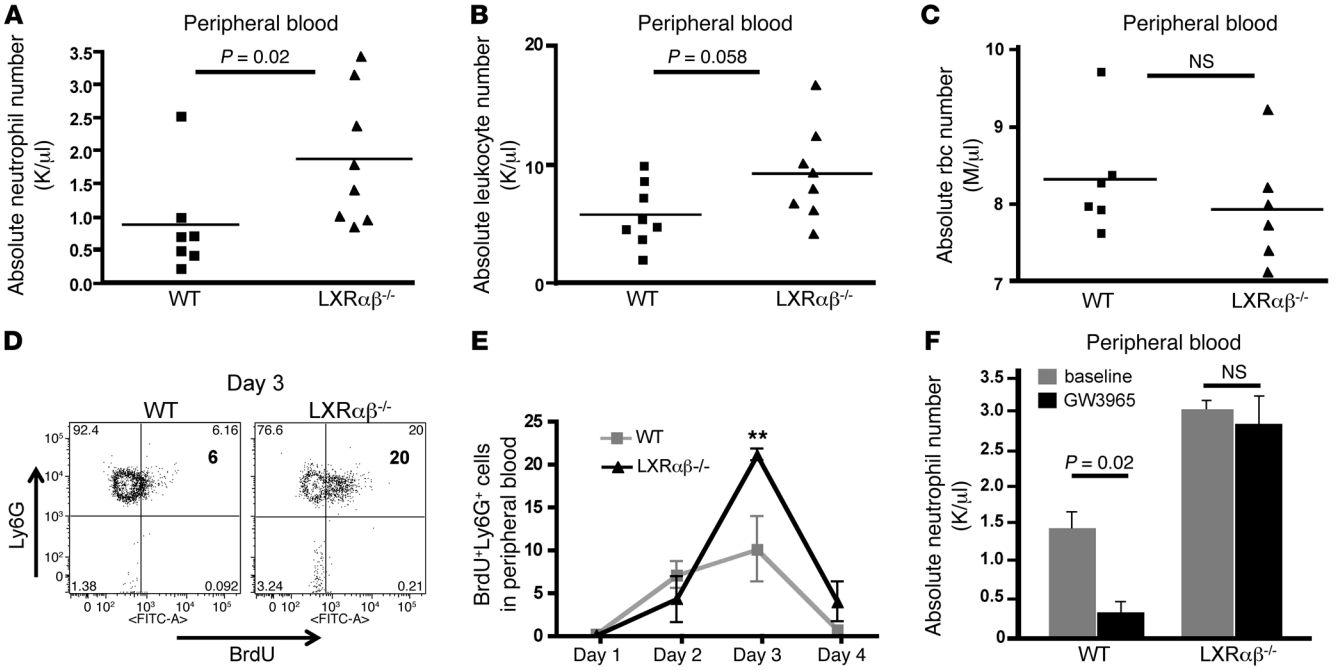

Figure 1
LXR signaling regulates neutrophil homeostasis. (**A**–**C**) Absolute neutrophil (**A**), leukocyte (**B**), and rbc (**C**) counts in peripheral blood of 6- to 8-week-old WT and LXRαβ$^{-/-}$ mice. Each point represents an individual mouse. *P* values are shown. (**D**) Representative FACS plots of Ly6G^{hi}BrdU^{+} cells gated through CD11b^{+} in peripheral blood of 6- to 8-week-old WT and LXRαβ$^{-/-}$ mice on day 3 after BrdU injection (2 mg i.p.). Percent Ly6G^{hi}BrdU^{+} cells is indicated within plots. (**E**) Frequency of Ly6G^{hi} BrdU^{+} cells gated through CD11b^{+} in peripheral blood of 6- to 8-week-old WT or LXRαβ$^{-/-}$ mice on the indicated days after BrdU pulse. $n = 4$ per group. (**F**) Absolute number of neutrophils in peripheral blood of 6- to 8-week-old WT mice fed chow compounded with 0.012% GW3965 or control chow for 3.5 days. $n = 3$ per group. Data are representative of 2 experiments. $^{**}P < 0.01$.

Results

LXRs regulate neutrophil homeostasis in young mice. To assess the ability of LXR signaling to impact neutrophil homeostasis, 6- to 8-week-old WT mice and *Nr1h3*$^{-/-}$*Nr1h2*$^{-/-}$ mice (referred to herein as LXRαβ$^{-/-}$) were injected i.p. with PBS or 3% thioglycolate (26). After 3 hours, peritoneal fluid was collected, and the composition of the lavage was assessed by flow cytometry (Supplemental Figure 1A; supplemental material available online with this article; doi:10.1172/JCI58393DS1). As expected, the cell populations in lavage fluid from WT and LXRαβ$^{-/-}$ mice injected with PBS contained less than 1% neutrophils (defined as GR-1^{hi}CD11b^{hi}MHC class II^{-}; Supplemental Figure 1B). Thioglycolate-challenged WT and LXRαβ$^{-/-}$ mice showed similar increases in neutrophil composition of the lavage fluid (Supplemental Figure 1B), consistent with normal extravasation of LXRαβ$^{-/-}$ neutrophils into the peritoneal space.

Unexpectedly, complete blood counts (CBCs) revealed a modest leukocytosis in LXRαβ$^{-/-}$ mice, characterized by a 2-fold increase in circulating neutrophils (Figure 1, A and B, and Supplemental Figure 2A). Peripheral rbc counts from LXRαβ$^{-/-}$ mice were normal (Figure 1C), and no significant differences in metamyelocytes or band cells were noted on histological examination of peripheral blood smears (data not shown), which indicates that circulating neutrophils in LXRαβ$^{-/-}$ mice are mature.

To test whether LXR signaling influences neutrophil homeostasis, WT and LXRαβ$^{-/-}$ mice were pulsed with a single injection of BrdU, and the frequency of Ly6G^{+}GR-1^{hi}CD11b^{hi}BrdU^{+} cells was assessed in peripheral blood for 4 days (27). Fluorescence-activated cell sorting (FACS) analysis revealed that the frequency of circulating BrdU^{+} neutrophils in WT mice peaked on day 3 at approximately 10% of total Ly6G^{+}GR-1^{hi}CD11b^{hi} cells and returned to background staining by day 4 (Figure 1, D and E, and Supplemental Figure 2B). In contrast, circulating BrdU^{+} neutrophils from LXRαβ$^{-/-}$ mice represented greater than 21% of total neutrophils in peripheral blood on day 3 ($P < 0.01$; Figure 1, D and E). Moreover, a substantial population of BrdU^{+} neutrophils (4% of total Ly6G^{+}GR-1^{hi}CD11b^{hi} cells) remained detectable in the circulation on day 4 (Figure 1E and Supplemental Figure 2B). Thus, LXR signaling regulates the number of neutrophils released from bone marrow into the circulation and affects neutrophil turnover.

We next sought to determine whether global activation of LXR exerts an opposite effect on circulating neutrophil counts. The synthetic LXR agonist GW3965 (28) was administered to WT C57BL/6 mice for 3 days, and CBCs were performed. Strikingly, GW3965 administration suppressed circulating neutrophil counts in WT mice ($P = 0.02$, Figure 1F), but had no effect in LXRαβ$^{-/-}$ mice. Taken together, these data indicate that both gain and loss of LXR activity affects peripheral neutrophil homeostasis.

Genetic deletion of LXR does not intrinsically alter neutrophil development or survival. We initially considered that LXR might intrinsically affect granulopoietic cell development or lineage commitment. To formally address this possibility, we performed CFU assays on whole bone marrow from WT and LXRαβ$^{-/-}$ mice. Phenotypic and quantitative assessment of plates on days 8–12 revealed no

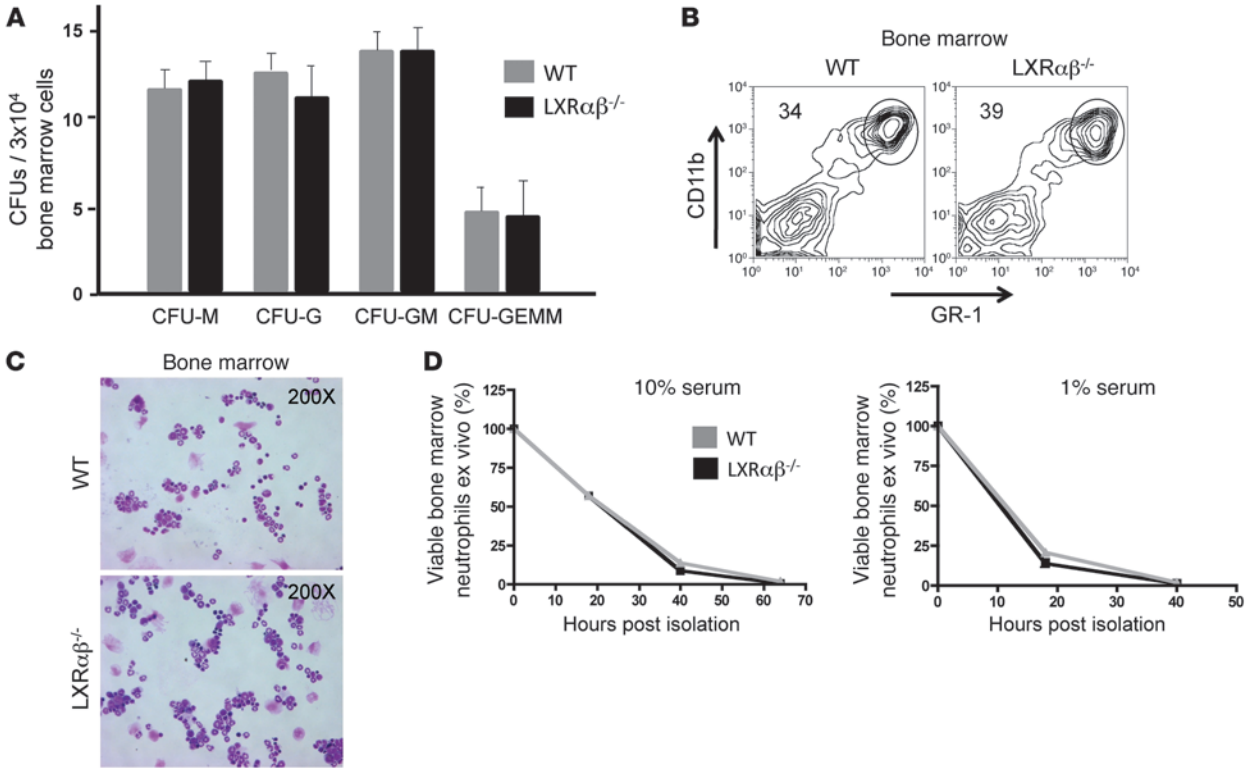

Figure 2

LXR does not intrinsically influence granulocyte development and survival. (**A**) Quantification of monocytic (CFU-M), granulocytic (CFU-G), mixed granulocytic/monocytic (CFU-GM), and mixed granulocytic/erythroid/monocytic/megakaryocytic (CFU-GEMM) bone marrow colonies formed per 3×10^4 WT and LXRαβ$^{-/-}$ nucleated bone marrow cells on day 8 using standard differentiation conditions. Colonies were counted and analyzed by color and morphology to assign category. Data are representative of 2 experiments performed in triplicate. (**B**) FACS analysis of CD11b^{hi}GR-1^{hi} cells in bone marrow of 6- to 8-week-old WT and LXRαβ$^{-/-}$ mice. FACS data are representative of greater than 10 mice. (**C**) H&E stains of purified CD11b^{hi}GR-1^{hi} cells in bone marrow of 6- to 8-week-old WT and LXRαβ$^{-/-}$ mice. Original magnification, ×200. (**D**) Frequency of viable (PI-negative, annexin V–negative) purified bone marrow neutrophils cultured in media with 10% or 1% FBS for 18, 40, and 64 hours. Data are representative of 2 experiments performed in triplicate.

significant differences in the quantity, morphology, or phenotype of granulopoietic colonies formed under standard differentiation conditions (Figure 2A). FACS analysis revealed no significant difference in the frequency of GR-1^{hi}CD11b^{hi} myeloid cells in the bone marrow of young LXRαβ$^{-/-}$ compared with control mice (Figure 2B). Similarly, no difference in granulocyte precursors was noted in peripheral smears (Figure 2C). Thus, the leukocytosis noted in CBCs of LXRαβ$^{-/-}$ mice did not appear to result from a requirement for LXR signaling during granulopoiesis.

An alternative possibility is that the increased number of neutrophils we observed in LXRαβ$^{-/-}$ mice reflects differences in neutrophil life span (1–5). Neutrophils were purified to greater than 95% from bone marrow and cultured in media containing 10% or 1% serum. No difference in the number of dead LXRαβ$^{-/-}$ and WT neutrophils was noted at 18 or 40 hours, either in complete media or under proapoptotic conditions (Figure 2D). These data suggest that LXR signaling in the neutrophil itself does not intrinsically affect cell survival.

No evidence for a generalized proinflammatory state in young LXRαβ$^{-/-}$ mice. LXRs have established roles in controlling inflammatory gene expression (17, 18). Therefore, it is possible that the increase in circulating neutrophil numbers we observed in LXRαβ$^{-/-}$ mice is a consequence of chronic inflammatory cytokine expression. Serum from young 6- to 8-week-old WT and LXRαβ$^{-/-}$ mice was collected, and the circulating levels of inflammatory cytokines were determined by Luminex assays. Importantly, no significant difference in circulating inflammatory/neutrophilic cytokine levels was noted in these young mice (Supplemental Figure 3A). Consistent with our recent report that LXRαβ$^{-/-}$ mice acquire an age-dependent lupus-like disease (29), 9-month-old LXRαβ$^{-/-}$ mice showed derangement in a broad array of cytokines involved in inflammatory and allergic immune responses (Supplemental Figure 3B). Nevertheless, the lack of evidence for alterations in circulating inflammatory cytokines in young LXRαβ$^{-/-}$ mice argues against generalized inflammation being the basis of the neutrophil phenotype.

Accumulation of apoptotic neutrophils in spleen and liver of LXRαβ$^{-/-}$ mice. Our BrdU labeling data indicated that LXR signaling affects neutrophil turnover. Senescent neutrophils are primarily cleared from the circulation by tissue phagocytes in the liver, spleen, and bone marrow (8, 10). As we did not observe a difference in the bone marrow compartment, we examined the spleen and liver of young LXRαβ$^{-/-}$ mice for evidence of accumulating neutrophils. Consistent with previous reports (29), loss of LXR did not affect total nucleated cell numbers in spleen (Supplemental Figure 4A). Analysis of spleen,

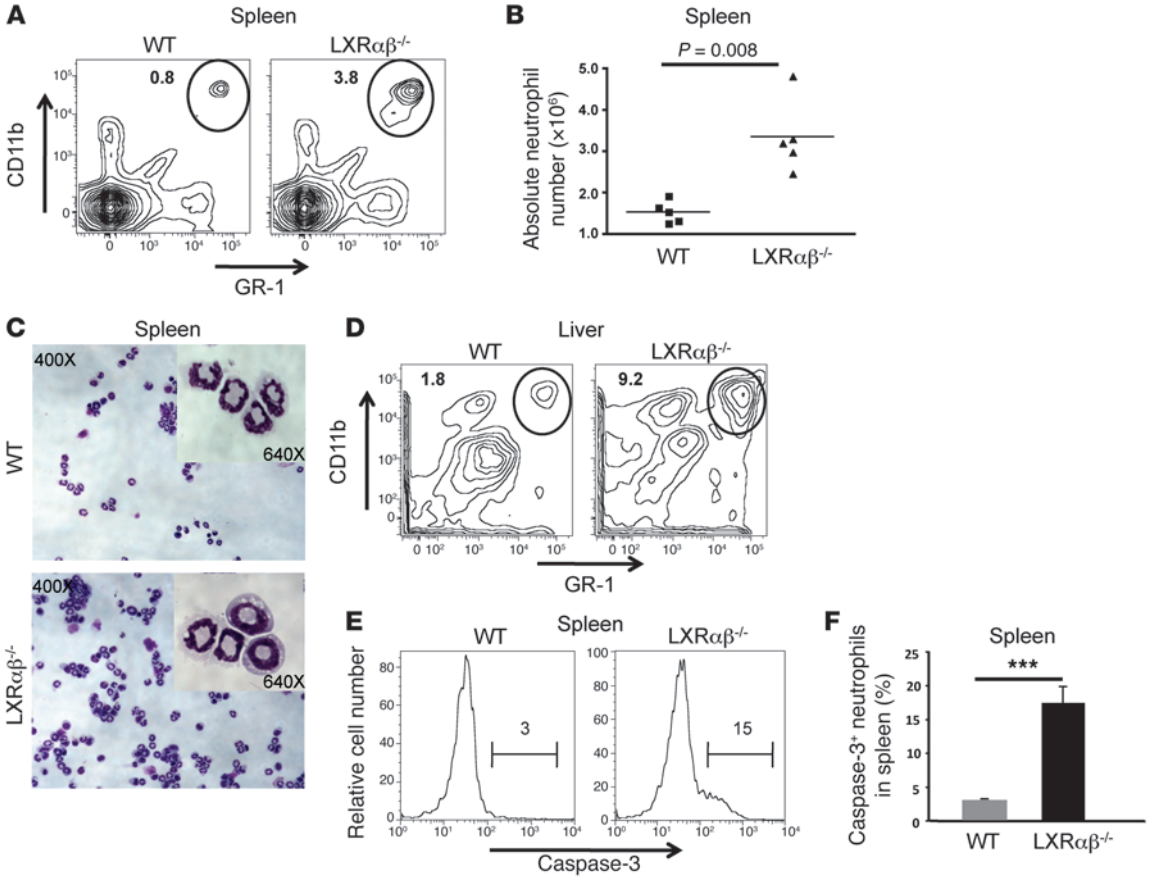

Figure 3

Accumulation of neutrophils in spleen and liver of LXRαβ$^{-/-}$ mice. (**A** and **B**) FACS analysis and absolute numbers of CD11b^{hi}GR-1^{hi} cells in spleen of 6- to 8-week-old WT and LXRαβ$^{-/-}$ mice. (**A**) Percent cells in the circled region is indicated in each plot. (**B**) Each point represents an individual mouse. (**C**) H&E stains of FACS-sorted CD11b^{hi}GR-1^{hi} cells in spleen of 6-week-old WT and LXRαβ$^{-/-}$ mice. Original magnification, ×400, ×640 (insets). (**D**) FACS plot of CD11b^{hi}GR-1^{hi} cells in liver parenchyma from WT and LXRαβ$^{-/-}$ mice. Liver was perfused with saline and then collagenase for 5 minutes each prior to harvesting tissue. Percent cells in the circled region is indicated in each plot. (**E** and **F**) Expression and frequency of intracellular cleaved caspase-3 in splenic GR-1^{hi}CD11b^{hi} cells gated through MHC class II^{-} cells. Numbers in **E** denote intracellular cleaved caspase-3 frequency in the bracketed regions. FACS plots are representative of 8 mice. ***$P < 0.001$.

liver, and LN from LXRαβ$^{-/-}$ mice consistently revealed a 3- to 10-fold increase in the frequency of GR-1^{hi}CD11b^{hi}MHC class II^{-} cells as well as their absolute numbers ($P = 0.008$) compared with WT mice (Figure 3, A, B, and D, and Supplemental Figure 4B). The accumulation of neutrophils was not a generalized process in LXRαβ$^{-/-}$ tissues, as we did not find evidence of proinflammatory cytokines or neutrophilic infiltrates in nonlymphoid compartments, such as the peritoneal cavity or skin (Supplemental Figure 1B and Supplemental Figure 6C). Loss of both LXRα and LXRβ appeared to be required for alterations in neutrophil homeostasis, because CBCs from age-matched LXRα and LXRβ single-knockout mice were no different from their WT counterparts, and an accumulation of GR-1^{hi}CD11b^{hi}MHC class II^{-} cells was not observed in spleen of LXRα or LXRβ single-knockout mice (Supplemental Figure 4, C–E).

GR-1 and CD11b can be variably expressed on both myeloid and monocytic lineages (30). Thus, we also examined these cells for expression of the alternative neutrophil markers Ly6G or MCA771 (30, 31). We found an equivalent increase in Ly6G^{+}CD11b^{hi}MHC class II^{-} cells and MCA771^{hi}CD11b^{hi}MHC class II^{-} cells in spleens of LXRαβ$^{-/-}$ mice (Supplemental Figure 5A). To confirm that the cells accumulating in LXRαβ$^{-/-}$ mice were bona fide neutrophils, splenic CD11b^{hi}GR-1^{hi} cells were subjected to FACS. H&E staining of splenic CD11b^{hi}GR-1^{hi} FACS-sorted cells demonstrated that these cells were enriched for mature PMNs (Figure 3C). We also considered the possibility that the accumulation of GR-1^{hi}CD11b^{hi}MHC class II^{-} cells in spleen is a function of increased extramedullary hematopoiesis. However, CFU assays revealed little difference in hematopoietic potential between WT and LXRαβ$^{-/-}$ splenocytes (Supplemental Figure 5B).

Activation of neutrophils alters the expression pattern of CD11b and CD62L. Phenotypic examination of SSC^{hi}GR-1^{hi} cells in LXRαβ$^{-/-}$ spleen and LN demonstrated that these cells expressed WT levels of CD62L and CD11b (Supplemental Figure 6A). These findings suggested that the neutrophils in periphery of young LXRαβ$^{-/-}$ mice were likely in a quiescent state. FACS analysis further revealed an approximately 5-fold increase in intracellular cleaved caspase-3 in LXRαβ$^{-/-}$ splenic GR-1^{+}CD11b^{+} cells compared with control WT splenic cells ($P < 0.001$, Figure 3, E and F). Taken together, these data indicate that LXRαβ$^{-/-}$ mice accumulate increased numbers of apoptotic neutrophils in spleen.

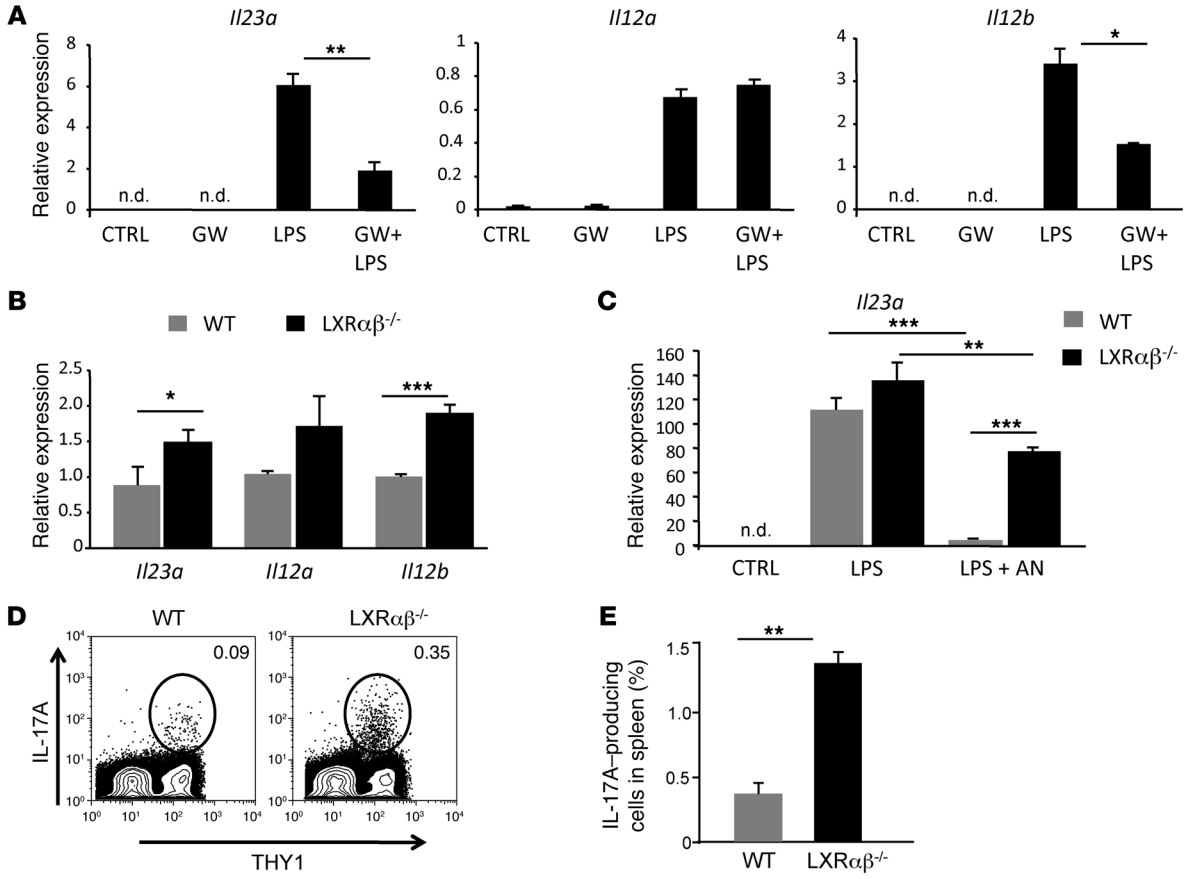

Figure 4

LXR signaling regulates the IL-23/IL-17 granulopoietic signaling axis. (**A**) *Il23a*, *Il12a*, and *Il12b* expression in WT BMDCs treated with LPS and GW3965. On day 7, BMDCs were treated with 1 μM GW3965 or vehicle for 18 hours and then activated with 1 ng/ml LPS for 5 hours. (**B**) Basal *Il23a*, *Il12a*, and *Il12b* expression in WT and LXRαβ$^{-/-}$ BMDCs. (**C**) *Il23a* gene expression in WT and LXRαβ$^{-/-}$ thioglycolate-elicited macrophages activated with 1 ng/ml LPS for 5 hours and cocultured with purified aged neutrophils (AN). Experiments are representative of 2–4 experiments performed in triplicate. (**D** and **E**) Frequency of IL-17A^{+} WT and LXRαβ$^{-/-}$ T cells in spleen from 6- to 8-week-old mice. Cells were stimulated with PMA/ionomycin in the presence of brefeldin A for 5 hours ex vivo. Cells were stained with anti-Thy1, fixed, permeabilized, stained with anti–IL-17A, and analyzed by flow cytometry. Percent Thy1^{+}IL-17^{+} cells in spleen is indicated. FACS plots are representative of 4 mice per group repeated twice. $^{*}P < 0.05$, $^{**}P < 0.01$, $^{***}P < 0.001$.

LXR signaling regulates the IL-23/IL-17 granulopoietic signaling axis. The IL-23/IL-17 cytokine signaling cascade plays a critical role in regulating neutrophilic responses (10, 12, 32). Secretion of IL-23 from DCs and macrophages induces IL-17 production from IL-23 receptor–bearing T lymphocytes (33). In turn, IL-17 induces stromal cells in the bone marrow to produce G-CSF, resulting in the release of mature neutrophils into the circulation (13). To test whether LXR signaling regulates the IL-23/IL-17 granulopoietic cytokine axis, we cultured WT myeloid bone marrow–derived DCs (BMDCs) in low-serum conditions to reduce background LXR activity. Cultures were then treated with GW3965 or vehicle for 18 hours and activated with LPS. After 5 hours of LPS activation, mRNA was collected, and gene expression was analyzed by real-time PCR. Unstimulated DCs produced little *Il23a*, *Il12a*, or *Il12b* mRNA, and LPS stimulation robustly induced their expression (Figure 4A). Remarkably, activation of LXR with GW3965 strongly reduced *Il23a* and *Il12b* expression, but had little effect on *Il12a* expression. We next asked whether IL-23 expression is dysregulated in the absence of LXR signaling. mRNA from WT and LXRαβ$^{-/-}$ myeloid BMDCs was collected on day 7 of culture, and basal expression of *Il23a* and *Il12b* was indeed higher in LXRαβ$^{-/-}$ myeloid BMDCs than in the WT counterparts (Figure 4B).

Phagocytosis of neutrophils has previously been shown to repress inflammatory gene expression in APCs (10). Thus, we asked whether apoptotic neutrophils modulate *Il23a* gene expression in an LXR-dependent manner. Thioglycolate-elicited WT and LXRαβ$^{-/-}$ macrophages were stimulated with LPS and cocultured with apoptotic WT neutrophils. As expected, engulfment of apoptotic neutrophils significantly decreased LPS-induced *IL23a* expression in WT macrophages ($P < 0.001$, Figure 4C). The antiinflammatory effect of apoptotic neutrophils was markedly reduced in the absence of LXR ($P < 0.01$, Figure 4C). These data indicate that LXR mediates tolerogenic signals generated from phagocytosis of neutrophils in APCs.

A logical prediction originating from our data is that basal IL-17A production from T cells should be constitutively elevated in LXRαβ$^{-/-}$ mice. To test this prediction, we examined ex vivo cytokine production from WT and LXRαβ$^{-/-}$ splenic T cells iso-

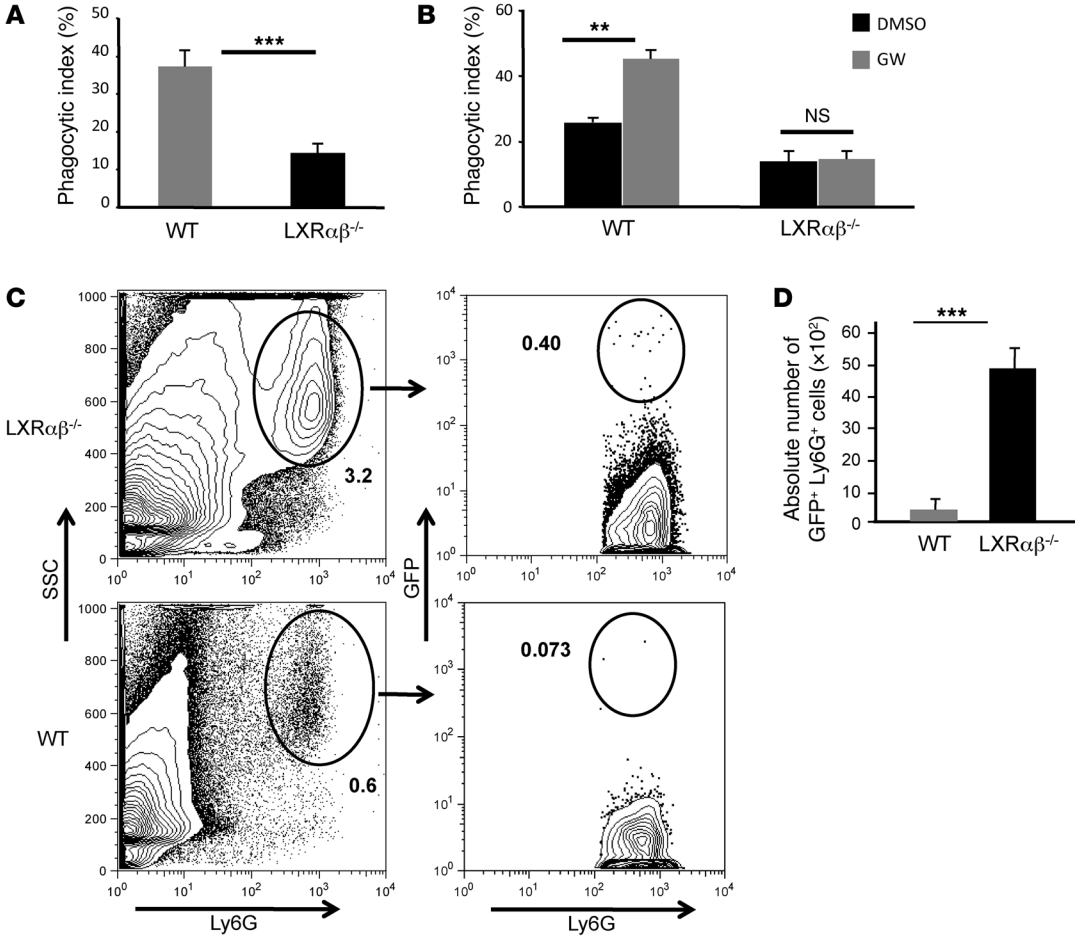

Figure 5

LXR regulates phagocytosis of aged neutrophils in vitro and clearance in vivo. (**A**) Decreased phagocytosis of apoptotic neutrophils by LXRαβ$^{-/-}$ macrophages. Thioglycolate-elicited, aged peritoneal WT neutrophils were labeled with CMFDA (cell tracker green) and cocultured with thioglycolate-elicited macrophages (labeled red with CMPTX) for 90 minutes. Cultures were extensively washed with cold PBS and enzyme free cell dissociation buffer to remove non- and semiadherent neutrophils. Quantification of engulfed neutrophils was determined by confocal microscopy. In vitro engulfment assays are a composite of 5 individual experiments performed in triplicate. (**B**) LXR signaling promoted phagocytosis of apoptotic neutrophils. WT and LXRαβ$^{-/-}$ macrophages were pretreated with GW3965 (1 μM) for 18 hours and then cultured with apoptotic neutrophils as above. (**C** and **D**) In vivo clearance of purified lysM-EGFP^{+} bone marrow neutrophils from spleen of WT and LXRαβ$^{-/-}$ mice 40 hours after adoptive transfer. Percent GFP^{+}Ly6G^{+} cells in total spleen is indicated. GFP neutrophil counts were computed by determining total nucleated splenocyte counts and multiplying by the frequency of GFP^{+}Ly6G^{+} cells. In vivo neutrophil clearance FACS plots are representative of 4 mice. $^{**}P < 0.01$, $^{***}P < 0.001$.

lated from 6- to 8-week-old mice. Strikingly, intracellular staining revealed that approximately 5-fold more splenic LXRαβ$^{-/-}$ T cells were producing IL-17A than were their WT counterparts ($P < 0.01$, Figure 4, D and E). To rule out the possibility that the increased frequency of IL-17–producing T cells in LXRαβ$^{-/-}$ T cells reflected an increased inflammatory state in the spleen, we also examined IFN-γ and IL-2 expression. However, we observed no difference in the frequency of IFN-γ– or IL-2–expressing WT and LXRαβ$^{-/-}$ T cells ex vivo (Supplemental Figure 6B). Thus, the increased frequency of IL-17A–producing cells is likely to be a specific response rather than a reflection of generalized inflammation.

LXR signaling regulates phagocytosis of apoptotic neutrophils. Senescent neutrophils are cleared by phagocytes in the spleen, liver, and bone marrow (7, 8, 10). Thus, a deficiency in the frequency of tissue macrophages or DCs in LXRαβ$^{-/-}$ mice might translate into a reduced clearance of aged neutrophils. To address this possibility, we examined the expression of tissue macrophage–associated genes in liver and spleen. Surprisingly, we observed a significant increase in *Cd68*, *Emr1* (F4/80), and *Itgam* (CD11b) gene expression suggestive of an increased number of macrophages in liver and spleen of LXRαβ$^{-/-}$ mice (Supplemental Figure 7A). FACS analysis also demonstrated a trend toward increased numbers of DCs and macrophages in LXRαβ$^{-/-}$ splenocytes (Supplemental Figure 7B). Thus, the accumulation of apoptotic neutrophils in spleen and liver of LXRαβ$^{-/-}$ mice does not appear to be a function of decreased numbers of tissue macrophages and DCs. However, we cannot rule out the possibility that a specific subset of phagocytes is dysfunctional or absent in LXRαβ$^{-/-}$ mice.

We next asked whether LXR signaling regulates the capacity of macrophages to phagocytose apoptotic neutrophils. To address this, we cultured WT and LXRαβ$^{-/-}$ thioglycolate-elicited perito-

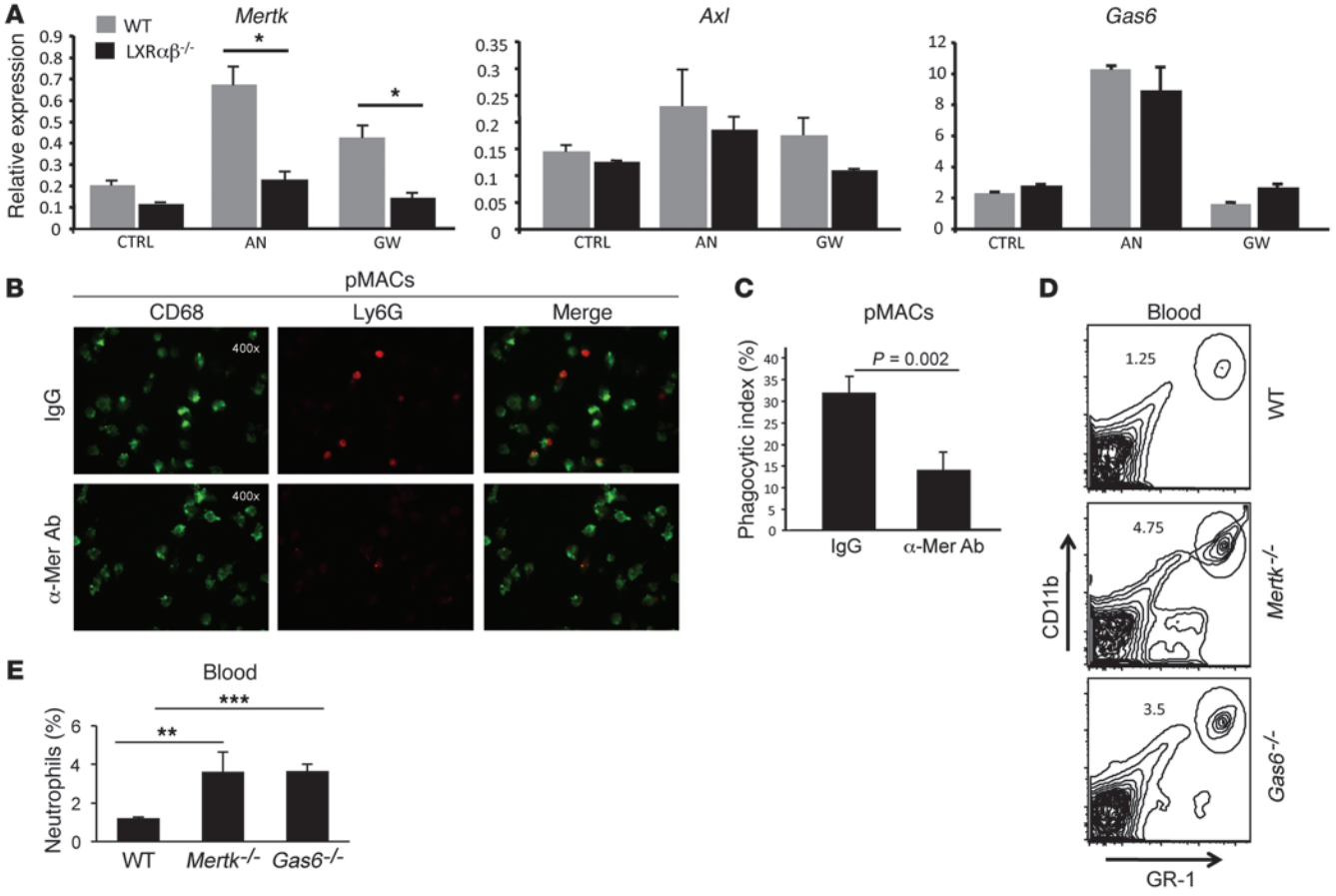

Figure 6

The LXR/MER axis regulates neutrophil clearance and homeostasis. (**A**) *Mertk*, *Gas6*, and *Axl* gene expression from WT and LXRαβ$^{-/-}$ thioglycolate-elicited peritoneal macrophages treated with GW3965 (1 μM) or cocultured with aged neutrophils for 18 hours. Data are representative of 3 experiments performed in triplicate. (**B** and **C**) Confocal microscopy images (**B**) and quantification of neutrophil phagocytosis (**C**). WT thioglycolate-elicited peritoneal macrophages were treated with control IgG or anti-Mer Ab and then cocultured with aged neutrophils for 90 minutes. Subsequently, cultures were extensively washed with cold PBS and enzyme free cell dissociation buffer to remove non- and semiadherent neutrophils. Cells were stained for CD68 expression and Ly6G expression to distinguish macrophages from neutrophils (original magnification, ×400), and the phagocytic index was determined. Data are representative of 3 experiments performed in triplicate. (**D** and **E**) Frequency of blood GR-1^{hi}CD11b^{hi} cells from 5- to 6-week-old WT, *Gas6*$^{-/-}$, or *Mertk*$^{-/-}$ mice. Percent cells in the circled region is indicated in each plot. FACS plots are representative of 4 mice per group.

neal macrophages with aged WT neutrophils for 90 minutes and quantified engulfment by confocal microscopy. As expected, WT macrophages engulfed a significant fraction of aged neutrophils, but LXRαβ$^{-/-}$ macrophages were far less efficient in their phagocytosis ($P < 0.001$, Figure 5A). In complementary experiments, we asked whether pharmacological activation of LXR could increase neutrophil uptake. WT macrophages were treated with GW3965 18 hours before challenge with aged neutrophils; after an additional 90 minutes, cells were analyzed to determine phagocytosis. Activation of LXR increased phagocytosis nearly 2-fold in WT macrophages, but not LXRαβ$^{-/-}$ macrophages ($P < 0.01$, Figure 5B), indicative of a receptor-dependent effect.

To determine whether this LXR-dependent mechanism of neutrophil clearance is operative in vivo, GFP^{+} neutrophils (34) were purified from bone marrow and immediately injected i.v. into WT and LXRαβ$^{-/-}$ mice. Mice were sacrificed 18 and 40 hours after transfer, and the number of Ly6G^{hi}CD11b^{hi}GFP^{+} cells in spleen and bone marrow was determined by flow cytometry. 18 hours after adoptive transfer, no significant difference in the frequency or number of GFP^{+} cells was observed in spleen (Supplemental Figure 8A). At 40 hours after adoptive transfer, few Ly6G^{hi}GFP^{+} cells were detectable in spleen of WT mice (Figure 5, C and D). In contrast, a significant number of GFP^{hi} and GFP$^{int/lo}$ cells was still detectable in LXRαβ$^{-/-}$ mice ($P < 0.001$, Figure 5, C and D). Interestingly, no difference in the frequency of GFP^{hi} cells was noted in WT and LXRαβ$^{-/-}$ bone marrow (Supplemental Figure 8B), which suggests that LXR signaling does not influence neutrophil clearance in bone marrow. Nevertheless, in combination with our BrdU labeling data, these results support the concept that LXR signaling affects the clearance of peripheral neutrophils in vivo. Moreover, these data strongly suggest that the accumulation of apoptotic neutrophils observed in the periphery of LXRαβ$^{-/-}$ mice is not the result of an intrinsic function of LXR in the neutrophil population.

Phagocytosis of aged neutrophils is dependent on the LXR/MER axis. The molecular events underlying the efficient clearance of senescent neutrophils by macrophages and DCs remain poorly defined. To determine whether phagocytosis of apoptotic neutrophils activates LXR, WT and LXRαβ$^{-/-}$ thioglycolate-elicited macrophages were fed purified aged neutrophils. After 90 minutes, unengulfed neutrophils were washed from cultures, and LXR target gene expression in adherent macrophages was determined. In untreated LXRαβ$^{-/-}$ macrophages, gene expression of *Mertk* was less than 50% that of WT controls (Figure 6A). Strikingly, engulfment of apoptotic neutrophils increased expression of the LXR target genes *Mertk* and *Abca1* (Figure 6A and Supplemental Figure 9A). An increase in the *Mertk* ligand *Gas6* was also observed in response to phagocytosis of aged neutrophils; however, this upregulation was not LXR dependent (Figure 6A). Upregulation of *Axl* was not observed in response to engulfment of apoptotic neutrophils, whereas *Tyro3* was not detectable in macrophages (Figure 6A). A similar expression pattern of TAM receptors was observed in myeloid BMDCs (Supplemental Figure 9B), which indicates that LXR signaling also influences expression of *Mertk* on myeloid DCs.

To directly test whether the Mer receptor mediates phagocytosis of apoptotic neutrophils, we cocultured thioglycolate-elicited WT macrophages or bone marrow–derived macrophages with apoptotic neutrophils in the presence of anti-Mer blocking antibodies. After 90 minutes, cultures were extensively washed and analyzed by confocal microscopy to determine the frequency of neutrophils engulfed by macrophages. Antibody blockade of Mer significantly reduced the phagocytosis of aged neutrophils by WT macrophages ($P = 0.002$, Figure 6, B and C; $P = 0.017$, Supplemental Figure 10).

Finally, our observation that engulfment of apoptotic neutrophils upregulated *Mertk* and *Gas6* expression led us to hypothesize that the Gas6/Mer axis affects peripheral neutrophil homeostasis. To address this, we examined spleen, peripheral blood, and bone marrow of 5-week-old *Mertk*$^{-/-}$ or *Gas6*$^{-/-}$ animals for alterations in neutrophil frequency. We observed a significant increase in the frequency of GR-1^{hi}CD11b^{hi} cells from peripheral blood and spleen, but not bone marrow (Figure 6, D and E, and Supplemental Figure 11), reminiscent of the phenotype of LXRαβ$^{-/-}$ mice. Importantly, these changes in neutrophil homeostasis developed before any observable alterations in peripheral immune cell composition were observed. Thus, the LXR/Mer/Gas6 phagocytic axis influences peripheral clearance of neutrophils in the absence of overt signs of systemic inflammation. Taken together, these data indicate that LXR plays a key role in regulating the engulfment of senescent neutrophils by controlling the processes of lipid efflux, phagocytosis, and granulopoietic cytokine gene expression in APCs.

Discussion

In the present study, we used complementary gain- and loss-of-function approaches to demonstrate that LXR signaling influences neutrophil homeostasis. We previously reported that LXRαβ$^{-/-}$ mice acquire age-dependent lymphadenopathy, splenomegaly, and lupus-like disease (29). Further analysis of young LXRαβ$^{-/-}$ mice (6–8 weeks old) here revealed markedly increased numbers of neutrophils in peripheral blood, spleen, and liver. We determined that the mechanism underlying this dysregulation was decreased peripheral clearance, rather than a difference in neutrophil production or survival. Our present data also indicated that LXRs play an important role in regulating neutrophil homeostasis through the control of the IL-23/IL-17 granulopoietic cytokine axis. Finally, we provided evidence that clearance of aged neutrophils in the periphery relies, at least in part, on LXR-dependent expression of the phagocytic receptor Mer and that genetic disruption of the Gas6/Mer axis also perturbs peripheral neutrophil numbers. Collectively, the data presented herein help to delineate molecular events controlling peripheral neutrophil homeostasis (Supplemental Figure 12). They also provide an additional physiological context in which to understand the dual functions of LXR nuclear receptors as regulators of both lipid metabolism and cytokine expression in APCs.

Several lines of evidence support the conclusion that the neutrophil phenotype in LXRαβ$^{-/-}$ mice is a function of decreased clearance by resident liver and splenic macrophages. LXRs did not intrinsically regulate neutrophil development in the bone marrow, as determined by CFU assays; however, BrdU uptake assays clearly demonstrated that LXR signaling regulated neutrophil turnover in vivo. Mechanistic studies revealed that LXRαβ$^{-/-}$ macrophages engulfed significantly fewer neutrophils than their WT counterparts. Conversely, LXR agonists increased the phagocytic capacity of WT neutrophils. Adoptive transfer of bone marrow neutrophils confirmed defective clearance by LXRαβ$^{-/-}$ macrophages in vivo. Finally, systemic administration of the LXR agonist GW3965 significantly reduced the frequency of circulating neutrophils in WT mice, but not LXRαβ$^{-/-}$ mice. LXRs have a well-defined antiinflammatory effect through the repression of inflammatory gene expression. Our data provide evidence that LXR signaling also plays a critical role in controlling immune cell homeostasis in the absence of overt inflammation.

A likely effector of LXR signaling on neutrophil clearance is the apoptotic cell receptor Mer, which we have previously shown to be a transcriptional target of LXR (29). Antibody blockade of Mer receptor significantly diminished the engulfment of aged neutrophils in macrophages. These data are consistent with recent reports using human and mouse systems (35, 36). Interestingly, phagocytosis of apoptotic neutrophils upregulated expression of *Mertk* and its ligand partner, *Gas6*, but had no effect on expression of other TAM receptors in macrophages. Importantly, upregulation of *Mertk* in response to neutrophil engulfment was LXR dependent. These data suggest that tonic signaling through the LXR/Mer axis is required to control peripheral neutrophil homeostasis. Indeed, examination of mice deficient in Mer or Gas6 revealed similarly increased numbers of neutrophils in the circulation and spleens of young mice.

However, it was clear that the majority of neutrophil clearance was preserved in mice deficient in LXR, Mer, or Gas6. Thus, additional phagocytic pathways are likely to be involved. In support of this concept, we observed no difference in the neutrophil counts from bone marrow of LXRαβ$^{-/-}$, *Mer*$^{-/-}$, or *Gas6*$^{-/-}$ mice, nor did we observe a difference in the accumulation of adoptively transferred neutrophils in the bone marrow of LXRαβ$^{-/-}$ mice (Supplemental Figure 8B). Given that the bone marrow is also an important site of aged neutrophil phagocytosis (37), we surmise that neutrophil clearance mechanisms occur in a tissue-specific manner. In the future, it will be of interest to examine other models of defective phagocytosis to determine the relevant receptor/ligand signaling axes involved in apoptotic neutrophil clearance.

Ley and colleagues have elegantly shown that clearance of peripheral neutrophils by phagocytes contributes to a feedback loop controlling bone marrow granulopoiesis (10). However, the mechanism by which phagocytosis influences granulopoietic

cytokine production is not well defined. Our present data indicate that LXR signaling is integral to this mechanism. Phagocytosis of neutrophils (and other apoptotic cells) activates LXRs, which in turn drive the expression of Mer. This positive feedback promotes the beneficial clearance of apoptotic neutrophils from peripheral tissues by macrophages. A second component of this model is the repression of the IL-23/IL-17 cytokine cascade. We showed here that LXR signaling downstream of apoptotic cell engulfment is critical for the repression of IL-23 expression. In the absence of LXR signaling, IL-23 was elevated, resulting in increased IL-17 expression from T cells.

Although LXRαβ$^{-/-}$ mice are known to develop generalized inflammation and frank autoimmune disease with age (29), our data suggest that the dysregulation of the IL-23/IL-17 cytokine axis is not likely to be secondary to generalized systemic inflammation in young LXRαβ$^{-/-}$ mice. We did not find evidence of proinflammatory gene expression in nonlymphoid compartments, such as skin (Supplemental Figure 6C), nor did we observe alterations in the frequency of IL-2– or IFN-γ–expressing T cells from spleen and LN of young LXRαβ$^{-/-}$ mice. Furthermore, phenotypic analysis of splenic and LN neutrophils did not reveal evidence of activation. Finally, we could not detect differences in the levels of circulating inflammatory cytokines, including IL-17, which suggests that the signals generated from peripheral tissues influencing neutrophil homeostasis circulate at exceedingly low levels. Thus, we conclude that the initial dysregulation of neutrophilic cytokine cascade in the peripheral lymphoid organs is a specific process, rather than a result of perturbations in inflammation control. Our data are consistent with defective neutrophil clearance being an early and perhaps primary defect in the evolution of autoimmunity in LXRαβ$^{-/-}$ mice. We hypothesize that as LXRαβ$^{-/-}$ mice age, the continued accumulation of senescent neutrophils may lead to loss of tolerance and development of a more generalized inflammatory process.

Our results may have substantial implications for understanding the pathogenesis of autoimmune disease. A prominent granulopoiesis gene signature has been reported in juvenile SLE patients (38), which suggests an important role for neutrophil homeostasis in the development of lupus. More recently, 2 important studies directly implicated the clearance of activated neutrophils in the pathogenesis of lupus (39, 40). These studies demonstrate that neutrophils isolated from lupus patients have a higher propensity to release extracellular DNA, also known as neutrophil extracellular traps (NETs), resulting in TLR9-dependent IFN-α production from host plasmacytoid DCs. NETs also contained an array of self-proteins (e.g., HMGBI and LL37) that play a role in augmenting inflammatory responses and have been directly implicated in the loss of self-tolerance. These data clearly indicate that neutrophils play an important role in SLE pathogenesis. We contend that even a modest defect in the clearance of peripheral neutrophils would lead to a significant number of neutrophils accumulating in the spleen and other peripheral lymphoid tissues. The accumulation of neutrophils undergoing cell death in close proximity to immune cells will likely have substantial consequences for activation of host APCs and self-tolerance. Thus, our prior description of an autoimmune disease phenotype in LXRαβ$^{-/-}$ mice (29) fits well with a role for LXR in neutrophil clearance. Future studies must address whether dysregulation of neutrophil homeostasis is a common early feature of models of SLE and the potential for LXR signaling to modify disease pathogenesis.

Methods

Media, reagents, and antibodies. The LXR agonist GW3965 (28) was provided by T. Willson and J. Collins (GlaxoSmithKline, Research Triangle Park, North Carolina, USA). Ligands were dissolved in dimethyl sulfoxide before use in cell culture. LXR ligands were used at 1 μM for in vitro experiments or 0.012% compounded in chow for in vivo experiments.

Flow cytometry. Single-cell suspensions from bone marrow, blood, or spleen were depleted of rbcs using hypotonic lysis. Cells were resuspended in PBS with 0.2% BSA and 0.1% sodium azide (Facs Buffer). Single cell suspensions were incubated for 10 min with anti-CD16/32 (Fc block), and stained for 30 minutes at 4°C. DAPI, 7-AAD, anti-mouse GR-1 (RB6-8C5), Ly-6G (1A8), CD4 (RM4-5), CD8 (53-6.7), CD11b (M1/70), CD11c (N418), CD19 (ID3), CD62L (MEL-14), MHC class II (M5/114), active caspase-3, IL-17 (TC11-18H10) Th1.2 (53-2.1) were purchased from BD Biosciences, eBioscience, or Biolegend. Cells were analyzed on FACSCalibur or LSR II (Becton Dickinson) with FlowJo software (Treestar).

RNA isolation and analysis. Total RNA was isolated from tissues using TRIzol (Invitrogen). 1 μg total RNA was reverse transcribed with random hexamers using the Taqman Reverse Transcription Reagents Kit (Applied Biosystems). Sybergreen (Diagenode or Roche) real-time quantitative PCR assays were performed using an Applied Biosystems 7900HT sequence detector or Roche Light cycler 480 II. Results show averages of at least duplicate experiments normalized to 36B4. Primer sequences are listed in Supplemental Table 1.

Animals. All animals were housed in a temperature-controlled room under a 12-hour light/12-hour dark cycle and under pathogen-free conditions. LXR-sufficient *Nbr1h3*$^{+/+}$*Nbr1h2*$^{+/+}$ mice and the LXR-deficient single-knockout *Nbr1h3*$^{-/-}$ and *Nbr1h2*$^{-/-}$ and double-knockout LXRαβ$^{-/-}$ (*Nbr1h3*$^{-/-}$*Nbr1h2*$^{-/-}$) mice on a C57BL/6 background (originally provided by D. Mangelsdorf, University of Texas Southwestern Medical Center, Dallas, Texas, USA) were greater than 10 generations backcrossed to C57BL/6. In some experiments, C57BL/6 mice were purchased from Jackson Laboratories. *Mertk*$^{-/-}$ (41) and *Gas6*$^{-/-}$ (42) mice were backcrossed 10 generations to C57BL/6. Control C57BL/6 animals for the experiment involving *Mertk*$^{-/-}$ and *Gas6*$^{-/-}$ animals were housed at Temple University (Philadelphia, Pennsylvania, USA); all others were housed at UCLA. For ligand treatment studies in vivo, mice were fed chow with either vehicle or 0.012% GW3965 for 3–4 days. LysM-EGFP mice (34) were originally provided by T. Graf (Albert Einstein University, New York, New York, USA).

Blood and serum analysis. For serum cytokine studies, blood was extracted through lethal cardiac puncture, then centrifuged at 5,510 *g* for 5 minutes in CapiJect tubes (Terumo Medical Corp.) to separate the serum. Serum cytokines were analyzed using Luminex protein assays and associated kits (MCYTO-70K; Millipore). For CBCs, 100 μl blood was collected by retro-orbital bleed, and CBCs were performed at UCLA's Division of Laboratory Animal Medicine using a Hemavet (Drew Scientific).

Adoptive transfer studies. Mice expressing eGFP^{+} neutophils (lysM-EGFP) were isolated from bone marrow as in *Cell culture*. Cells were stained for Ly6G and analyzed by FACS to confirm purity greater than 95% and immediately injected into mice intravenously (5×10^6 cells). Spleen and bone marrow were harvested at 18 and 40 hours after injection. Single-cell suspensions were analyzed for Ly6G and EGP by flow cytometry to determine frequency of Ly6G^{+}EGP^{+} cells. Absolute numbers of eGFP^{+} cells was determined by multiplying cell frequency by total cell count.

Cell culture. Bone marrow–derived macrophages and thioglycolate-elicited (TG-elicited) peritoneal macrophages were obtained as described previously (43). Macrophages were cultured in RPMI or DMEM containing 10% FBS. For differentiation of DCs, primary murine bone marrow was harvested and cultured in RPMI 1640 supplemented with 10% FBS, 100 U/ml penicillin, 100 mg/ml streptomycin, 2 mM L-glutamine, 10 mM HEPES

(all Gibco; Invitrogen), 50 mM 2-ME (Sigma-Aldrich), and 10 ng/ml GM-CSF for 8 days. The cells were then stimulated with 2 μg/ml LPS (Sigma-Aldrich) to activate the cells.

To purify bone marrow neutrophils, single-cell suspensions were made by depletion techniques using magnetic beads (Miltenyi; MACS) and a master mix of antibodies, anti-CD5 (clone 53-7.3), anti-Ter119 (clone Ter 119), anti-F4/80 (clone 13-4801-81), anti-CD45R (clone RA3-6B2), anti-CD4 (L3T4) (clone GK1.5), CD117 (c-kit) (clone 2B8), all from eBioscience. Cells were stained for Ly6G expression to confirm purity greater than 95% by FACS.

To purify peritoneal exudate neutrophils, WT mice were injected with 3% thioglycolate i.p. 4–6 hours (26) after injection exudates were pooled, and neutrophils were magnetically sorted using a cocktail of anti-Gr1 and anti-CD11b antibodies following by anti-rat IgG microbeads (Miltenyi Biotech) according to manufacturer's protocol. The positively selected fraction was analyzed by flow cytometry resulting in at least 90% pure population.

Intracellular cytokine assay. Single-cell suspensions were incubated for 5 hours with phorbol ester (PMA 50 ng/ml) and calcium ionophore (ionomycin 1 μg/ml) in the presence of brefeldin A (2 μg/ml; BD Biosciences) ex vivo. Cells were stained for surface expression of Thy1, fixed, and permeabilized using Cytofix/Cytoperm kit (BD Biosciences) and stained for intracellular IFN-γ, IL-2, and IL-17 according to the manufacturer's protocol.

Neutrophil cell death assay. Neutrophils were purified from bone marrow as described in *Cell culture*. Cells were stained for Ly6G expression to confirm purity greater than 95%. Cells were cultured in media and 10% FBS as indicated. Cells counts were performed on a Nexelcom Cellometer optical imager using trypan blue exclusion or stained with PI and annexin V for FACS analysis.

Phagocytosis assays. Peritoneal exudate neutrophils were cultured in RPMI media supplemented with 5% FBS. After 24 hours, more than 75% cells underwent apoptosis, as assessed by flow cytometry by annexin V staining. Apoptotic neutrophils were labeled with CFMDA (Invitrogen), and neutrophils were cultured with macrophages at a 1:10 macrophage/neutrophil ratio. In vitro phagocytosis assay were performed as previously described (29). Briefly, primary peritoneal macrophages were recovered from mice injected with 3% thyoglycolate for 3 days or derived from bone marrow. Cells were pelleted and resuspended in RPMI (Cambrex) medium supplemented with 10% FCS (Lonza), and 5×10^5 cells were plated on sterile glass coverslips. After incubation with ATs, macrophages were gently washed several times with cold PBS and Cell Dissociation Buffer, Enzyme Free PBS-based (Invitrogen), to remove free apoptotic thymocytes as described previously (29) Cells were then fixed with 2% paraformaldehyde, and phagocytosis was scored with confocal fluorescent microscopy. The phagocytic index (number of cells ingested per total number of macrophages, expressed as a percentage; ref. 29) was used as a determinant of phagocytosis. In some studies, macrophages were treated with 1 μM GW3965 in RPMI supplemented with 0.5% FCS prior to addition of apoptotic cells, and phagocytosis assays were performed as described above in RPMI containing 10% FBS. Studies with Mertk blocking antibody were performed in WT and LXRαβ$^{-/-}$ macrophages as previously described (29). 50 μg/ml of anti-Mertk antibody (R&D Systems) was added to RPMI medium for 3 hours before phagocytosis assays. To image macrophages and neutrophils, cells were stained with CD68–Alexa Fluor 488 from Serotec and Ly6G-biotin (1A8) followed by SA–Alexa Fluor 594 staining.

Colony-forming assays. To determine the myeloerythroid potential of the bone marrow and spleen, tissues were mechanically dissociated, and 3×10^4 nucleated cells were plated on 1.5 ml methylcellulose with a cocktail of recombinant cytokines (SCF, IL-6, IL-3, and EPO; MethoCult 3434, Stem Cell Technologies) supplemented by TPO (5 ng/ml). Cultures were plated in triplicate. Colonies were scored based on cell size, color, and morphology on days 7–10.

In vivo BrdU labeling. BrdU labeling assays were performed as previously described (27). Briefly, BrdU (10 mg/ml in PBS; BD Biosciences) was given by a single i.p. injection (2 mg/mouse). Mice were bled retroorbitally on days 0, 1, 2, 3, and 4. The percentage of BrdU$^+$Ly6G$^+$ cells was determined by staining with APC-conjugated Ly6G antibody followed by fixation, permeabilization, and intracellular staining with a FITC-conjugated anti-BrdU antibody (BrdU Flow kit; BD Biosciences).

Statistics. Mann-Whitney tests were applied to determine statistical significance using PRISM (GraphPad) for comparison of 2 groups. 1-way ANOVA with Bonferroni post-testing was used for experiments with more than 2 groups; for time course experiments, 2-way ANOVA with Bonferroni post-testing at individual time points was used. All data are presented as mean ± SD except the in vivo BrdU labeling experiment (mean ± SEM). A P value less than 0.05 was considered statistically significant.

Study approval. All animal experiments were approved by the Institutional Animal Care and Research Advisory Committee of UCLA.

Acknowledgments

We are grateful to D. Mangelsdorf for the LXR-deficient mice. We thank T. Willson and J. Collins for GW3965. We thank Binghai Ling and Rima Boyadjian for technical support. Flow cytometry was performed in the UCLA Flow Cytometry Core Facility, supported by NIH grants CA-16042 and AI-28697. P. Tontonoz is an investigator of the Howard Hughes Medical Institute. This work was supported by grants from the NIH (RR021975 to S.J. Bensinger, HL066088 and HL30568 to P. Tontonoz), the Lupus Research Institute (to S.J. Bensinger), and the Spanish Ministry of I+D SAF2008-00057 (to A. Castrillo).

Received for publication April 7, 2011, and accepted in revised form October 24, 2011.

Address correspondence to: Steven Bensinger, Institute for Molecular Medicine, Department of Pathology and Laboratory Medicine, 36-120 Center For Health Sciences, Box 951735, Los Angeles, California 90095, USA. Phone: 310.825.9885; Fax: 310.267.6267; E-mail: sbensinger@mednet.ucla.edu. Or to: Peter Tontonoz, Howard Hughes Medical Institute, Department of Pathology and Laboratory Medicine, 6770 MacDonald Research Labs, Box 951662, Los Angeles, California 90095, USA. Phone: 310.206.4546; Fax: 310.267.0382; E-mail: ptontonoz@mednet.ucla.edu.

Noelia A-Gonzalez's present address is: Department of Epidemiology and Public Health, Yale University, New Haven, Connecticut, USA.

1. Athens JW, et al. Leukokinetic studies. IV. The total blood, circulating and marginal granulocyte pools and the granulocyte turnover rate in normal subjects. *J Clin Invest*. 1961;40:989–995.
2. Price TH, Dale DC. Neutrophil preservation: the effect of short-term storage on in vivo kinetics. *J Clin Invest*. 1977;59(3):475–480.
3. Basu S, Hodgson G, Katz M, Dunn AR. Evaluation of role of G-CSF in the production, survival, and release of neutrophils from bone marrow into circulation. *Blood*. 2002;100(3):854–861.
4. Suratt BT, Young SK, Lieber J, Nick JA, Henson PM, Worthen GS. Neutrophil maturation and activation determine anatomic site of clearance from circulation. *Am J Physiol Lung Cell Mol Physiol*. 2001;281(4):L913–L921.
5. Dancey JT, Deubelbeiss KA, Harker LA, Finch CA. Neutrophil kinetics in man. *J Clin Invest*. 1976;58(3):705–715.
6. Mauer AM, Athens JW, Ashenbrucker H, Cartwright GE, Wintrobe MM. Leukokinetic studies. II. A method for labeling granulocytes in vitro with radioactive diisopropylfluorophosphate (Dfp). *J Clin Invest*. 1960;39(9):1481–1486.
7. Furze RC, Rankin SM. The role of the bone marrow in neutrophil clearance under homeostatic conditions in the mouse. *FASEB J*. 2008;22(9):3111–3119.

8. Shi J, Gilbert GE, Kokubo Y, Ohashi T. Role of the liver in regulating numbers of circulating neutrophils. *Blood*. 2001;98(4):1226–1230.
9. Martin C, Burdon PC, Bridger G, Gutierrez-Ramos JC, Williams TJ, Rankin SM. Chemokines acting via CXCR2 and CXCR4 control the release of neutrophils from the bone marrow and their return following senescence. *Immunity*. 2003;19(4):583–593.
10. Stark MA, Huo Y, Burcin TL, Morris MA, Olson TS, Ley K. Phagocytosis of apoptotic neutrophils regulates granulopoiesis via IL-23 and IL-17. *Immunity*. 2005;22(3):285–294.
11. Ren Y, et al. Nonphlogistic clearance of late apoptotic neutrophils by macrophages: efficient phagocytosis independent of beta 2 integrins. *J Immunol*. 2001;166(7):4743–4750.
12. Forlow SB, Schurr JR, Kolls JK, Bagby GJ, Schwarzenberger PO, Ley K. Increased granulopoiesis through interleukin-17 and granulocyte colony-stimulating factor in leukocyte adhesion molecule-deficient mice. *Blood*. 2001;98(12):3309–3314.
13. Semerad CL, Liu F, Gregory AD, Stumpf K, Link DC. G-CSF is an essential regulator of neutrophil trafficking from the bone marrow to the blood. *Immunity*. 2002;17(4):413–423.
14. Janowski BA, Willy PJ, Devi TR, Falck JR, Mangelsdorf DJ. An oxysterol signalling pathway mediated by the nuclear receptor LXR alpha. *Nature*. 1996;383(6602):728–731.
15. Peet DJ, et al. Cholesterol and bile acid metabolism are impaired in mice lacking the nuclear oxysterol receptor LXR alpha. *Cell*. 1998;93(5):693–704.
16. Repa JJ, Mangelsdorf DJ. The role of orphan nuclear receptors in the regulation of cholesterol homeostasis. *Annu Rev Cell Dev Biol*. 2000;16:459–481.
17. Joseph SB, Castrillo A, Laffitte BA, Mangelsdorf DJ, Tontonoz P. Reciprocal regulation of inflammation and lipid metabolism by liver X receptors. *Nat Med*. 2003;9(2):213–219.
18. Ogawa S, et al. Molecular determinants of crosstalk between nuclear receptors and toll-like receptors. *Cell*. 2005;122(5):707–721.
19. Joseph SB, et al. Synthetic LXR ligand inhibits the development of atherosclerosis in mice. *Proc Natl Acad Sci U S A*. 2002;99(11):7604–7609.
20. Tangirala RK, et al. Identification of macrophage liver X receptors as inhibitors of atherosclerosis. *Proc Natl Acad Sci U S A*. 2002;99(18):11896–11901.
21. Joseph SB, et al. LXR-dependent gene expression is important for macrophage survival and the innate immune response. *Cell*. 2004;119(2):299–309.
22. Valledor AF, Hsu LC, Ogawa S, Sawka-Verhelle D, Karin M, Glass CK. Activation of liver X receptors and retinoid X receptors prevents bacterial-induced macrophage apoptosis. *Proc Natl Acad Sci U S A*. 2004;101(51):17813–17818.
23. Arai S, et al. A role for the apoptosis inhibitory factor AIM/Spalpha/Api6 in atherosclerosis development. *Cell Metab*. 2005;1(3):201–213.
24. Hindinger C, et al. Liver X receptor activation decreases the severity of experimental autoimmune encephalomyelitis. *J Neurosci Res*. 2006; 84(6):1225–1234.
25. McGeachy MJ, et al. The interleukin 23 receptor is essential for the terminal differentiation of interleukin 17-producing effector T helper cells in vivo. *Nat Immunol*. 2009;10(3):314–324.
26. Qureshi R, Jakschik BA. The role of mast cells in thioglycollate-induced inflammation. *J Immunol*. 1988;141(6):2090–2096.
27. Eash KJ, Means JM, White DW, Link DC. CXCR4 is a key regulator of neutrophil release from the bone marrow under basal and stress granulopoiesis conditions. *Blood*. 2009;113(19):4711–4719.
28. Collins JL, et al. Identification of a nonsteroidal liver X receptor agonist through parallel array synthesis of tertiary amines. *J Med Chem*. 2002;45(10):1963–1966.
29. A-Gonzalez N, et al. Apoptotic cells promote their own clearance and immune tolerance through activation of the nuclear receptor LXR. *Immunity*. 2009;31(2):245–258.
30. Taylor PR, Brown GD, Geldhof AB, Martinez-Pomares L, Gordon S. Pattern recognition receptors and differentiation antigens define murine myeloid cell heterogeneity ex vivo. *Eur J Immunol*. 2003;33(8):2090–2097.
31. Fleming TJ, Fleming ML, Malek TR. Selective expression of Ly-6G on myeloid lineage cells in mouse bone marrow. RB6-8C5 mAb to granulocyte-differentiation antigen (Gr-1) detects members of the Ly-6 family. *J Immunol*. 1993;151(5):2399–2408.
32. Schwarzenberger P, et al. IL-17 stimulates granulopoiesis in mice: use of an alternate, novel gene therapy-derived method for in vivo evaluation of cytokines. *J Immunol*. 1998;161(11):6383–6389.
33. Cua DJ, Tato CM. Innate IL-17-producing cells: the sentinels of the immune system. *Nat Rev Immunol*. 2010;10(7):479–489.
34. Faust N, Varas F, Kelly LM, Heck S, Graf T. Insertion of enhanced green fluorescent protein into the lysozyme gene creates mice with green fluorescent granulocytes and macrophages. *Blood*. 2000;96(2):719–726.
35. McColl A, et al. Glucocorticoids induce protein S-dependent phagocytosis of apoptotic neutrophils by human macrophages. *J Immunol*. 2009;183(3):2167–2175.
36. Feng X, Deng T, Zhang Y, Su S, Wei C, Han D. Lipopolysaccharide inhibits macrophage phagocytosis of apoptotic neutrophils by regulating the production of tumour necrosis factor alpha and growth arrest-specific gene 6. *Immunology*. 2011;132(2):287–295.
37. Furze RC, Rankin SM. Neutrophil mobilization and clearance in the bone marrow. *Immunology*. 2008;125(3):281–288.
38. Bennett L, et al. Interferon and granulopoiesis signatures in systemic lupus erythematosus blood. *J Exp Med*. 2003;197(6):711–723.
39. Lande R, et al. Neutrophils activate plasmacytoid dendritic cells by releasing self-DNA-peptide complexes in systemic lupus erythematosus. *Sci Transl Med*. 2011;3(73):73ra19.
40. Garcia-Romo GS, et al. Netting neutrophils are major inducers of type I IFN production in pediatric systemic lupus erythematosus. *Sci Transl Med*. 2011;3(73):73ra20.
41. Camenisch TD, Koller BH, Earp HS, Matsushima GK. A novel receptor tyrosine kinase, Mer, inhibits TNF-alpha production and lipopolysaccharide-induced endotoxic shock. *J Immunol*. 1999;162(6):3498–3503.
42. Angelillo-Scherrer A, et al. Deficiency or inhibition of Gas6 causes platelet dysfunction and protects mice against thrombosis. *Nat Med*. 2001;7(2):215–221.
43. Castrillo A, et al. Crosstalk between LXR and toll-like receptor signaling mediates bacterial and viral antagonism of cholesterol metabolism. *Mol Cell*. 2003;12(4):805–816.